

Immunological Multimetal Deposition for Rapid Visualization of Sweat Fingerprints**

Yayun He, Linru Xu, Yu Zhu, Qianhui Wei, Meiqin Zhang, and Bin Su*

Abstract: A simple method termed immunological multimetal deposition (iMMD) was developed for rapid visualization of sweat fingerprints with bare eyes, by combining the conventional MMD with the immunoassay technique. In this approach, antibody-conjugated gold nanoparticles (AuNPs) were used to specifically interact with the corresponding antigens in the fingerprint residue. The AuNPs serve as the nucleation sites for autometallographic deposition of silver particles from the silver staining solution, generating a dark ridge pattern for visual detection. Using fingerprints inked with human immunoglobulin G (hIgG), we obtained the optimal formulation of iMMD, which was then successfully applied to visualize sweat fingerprints through the detection of two secreted polypeptides, epidermal growth factor and lysozyme. In comparison with the conventional MMD, iMMD is faster and can provide additional information than just identification. Moreover, iMMD is facile and does not need expensive instruments.

Whenever a finger touches the surface of an object, materials on the protuberant ridges will be transferred to the surface, thus leaving a fingerprint.^[1] Since the late 19th century, the unique patterns of fingerprints have been used as a means to biometrically identify individuals in forensic investigations.^[2] However, in many cases the fingerprints are not directly visible to the bare eye (termed latent fingerprints), and require “development” to permit their visualization. Over the last century, there have been numerous reagents and methods explored for the development of latent fingerprints, such as powder dusting, multimetal deposition (MMD), superglue fuming, and fluorescent dyes.^[3]

Recently, there has been a renewed interest in fundamental research in this field, triggered in part by the possibility that apart from identification, a fingerprint can provide additional information about a person. For example, the fingerprint residues may contain many human metabolites with biomedical or diagnostic values, as well as exogenously doped species, such as explosives and illicit drugs.^[4] For this purpose, many chemical imaging techniques, including electrochemical surface plasmon resonance,^[5] mass spectrometry,^[6] Fourier-transform infrared spectroscopy,^[7] and Raman spectroscopy,^[8] have been employed because of their ability to visualize a fingerprint and detect chemicals at the same time. Moreover, methods based on biolabeling have attracted intense interest because of their good sensitivity and selectivity. Russell et al. utilized immunomagnetic beads for the detection of metabolites of illicit drugs in fingerprints.^[9] Wood et al. took advantage of aptamer-based reagents to detect the lysozyme in the residues and develop the latent fingerprints.^[10] Li et al. employed a nanoplasmonic method by using aptamer-bound gold nanoparticles to visualize fingerprints and detect the contact residues of cocaine.^[11] Very recently, Yuan et al. reported a novel technique that integrates the advantages of near infrared light mediated imaging and molecular recognition through aptamer-functionalized upconversion nanoparticles.^[12] However, most of these methods involved sophisticated or expensive instruments, or the influence from excitation light. In addition, few of the methods have been used to examine protein/peptide components that are present in sweat fingerprint residues originating from the eccrine glands. Herein we report a conceptually new implementation, immunological multimetal deposition (iMMD), by combining the conventional MMD and the immunoassay, for the detection of protein/polypeptide secretions in fingerprints by bare eyes.

MMD, which was introduced to the forensic field by Saunders, is a very sensitive method for visualizing latent fingerprints on porous and nonporous surfaces.^[13] The method involves treatment of the fingerprint sample with a solution containing gold nanoparticles (AuNPs) and then with a solution of silver physical developer. AuNPs preferentially adsorb to the fingerprint residues through electrostatic or hydrophobic interactions, and then serve as catalytic nucleating sites for metallic silver deposition, eventually amplifying a black fingerprint on a lighter background.^[13,14] Recently, MMD has also been performed in a reverse way by developing the substrate rather than the fingerprint residue, eventually achieving a negative image.^[15]

Different from conventional MMD, iMMD uses antibody-modified AuNPs (AuNPs/antibody conjugates; Scheme 1). That way, the adsorption of AuNPs occurs through the

[*] Y. He,^[†] L. Xu,^[†] Prof. B. Su
Institute of Microanalytical Systems
Department of Chemistry, Zhejiang University
Hangzhou 310058 (China)
E-mail: subin@zju.edu.cn
Homepage: <http://mypage.zju.edu.cn/binsu>

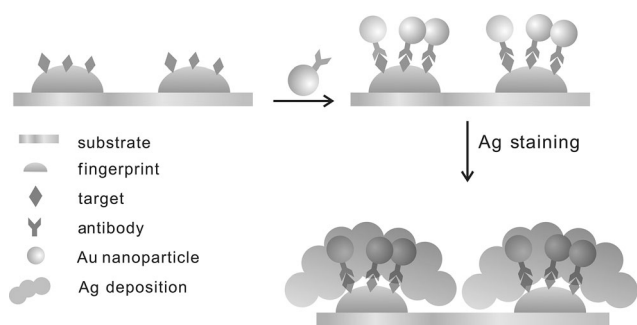
Y. Zhu, Q. Wei, Prof. M. Zhang
Research Center for Bioengineering and Sensing Technology
University of Science and Technology Beijing
Beijing 100083 (China)

[†] These authors contributed equally to this work.

[**] This work was supported by the National Natural Science Foundation of China (21222504, 21335001), the Zhejiang Provincial Natural Science Foundation (R14B050003), the Program for New Century Excellent Talents in University, and the Fundamental Research Funds for the Central Universities (2014XZZX003-04).

Supporting information for this article is available on the WWW under <http://dx.doi.org/10.1002/anie.201404416>.





Scheme 1. Illustration of an iMMD process, involving the binding of AuNPs/antibody conjugates to specific secretions and the enhancement by silver staining.

specific binding between the surface-tethered antibodies with the corresponding antigens in the fingerprint residues.^[16] Herein, we first evaluated and optimized the iMMD formulation through developing fingerprints inked with human immunoglobulin G (hIgG). Then, with this formulation, the visualization of latent fingerprints was successfully accomplished by the detection of two secretions, epidermal growth factor (EGF) and lysozyme, in the eccrine sweat residues.

Details regarding the collection and preparation of fingerprint samples, and operational details of the iMMD process are described in the Supporting Information. hIgG-inked fingerprints were obtained with 25 μL of a solution containing 0.1 mg mL^{-1} hIgG, unless otherwise specified. Various parameters, including the incubation time and temperature, the concentration of AuNPs/antibody conjugates, and the time required for silver physical development, were studied in order to optimize the method (Figures S1–S4). For example, the visual enhancement of the fingerprint ridges increased with the incubation time and silver staining time. However, in order to reduce the possibility of non-specific adsorption and background silver staining, both incubation and silver staining times were limited to 15 minutes. The optimized conditions for iMMD are summarized in Table 1; the whole iMMD process requires approximately 40 minutes.

Table 1: Optimized iMMD formulation.

Parameters	Optimized conditions
Incubation time	15 min
Incubation temperature	RT
Concentration of AuNPs/antibody conjugates	0.2 mg mL^{-1}
Time of silver staining	15 min

Figure 1a displays an hIgG-inked fingerprint developed by iMMD. The spatial pattern of the fingerprint is apparently enhanced, and the dark ridges contrast remarkably with the bright substrate. The enhancement can be semiquantitatively confirmed by comparing the cross-sectional gray value over a few papillary ridges. As shown in Figure 1b, the gray value varies insignificantly from ridge to furrow in the bright-field image, but strikingly in the iMMD-enhanced image, with an

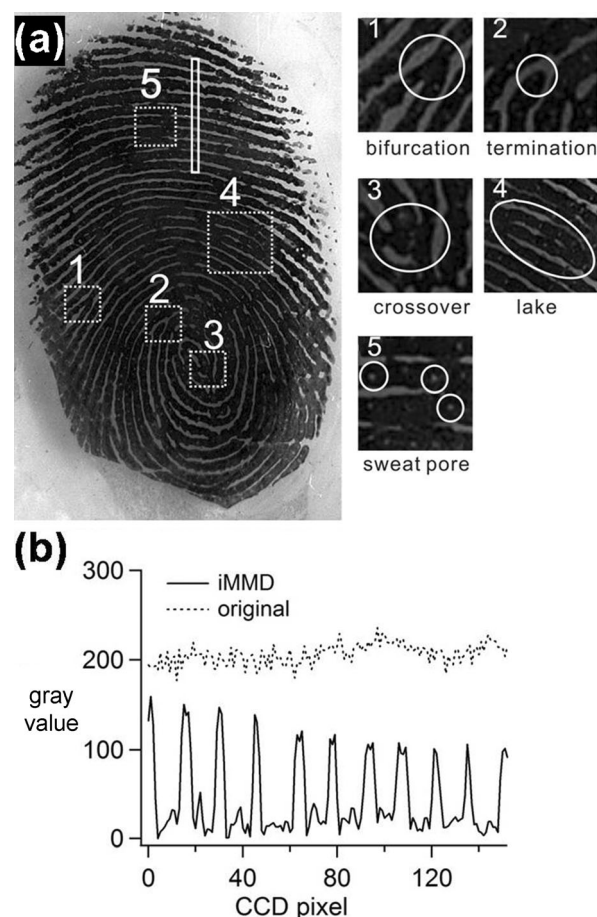


Figure 1. a) Optical image of an hIgG-inked fingerprint developed by iMMD, with various second-level details, such as bifurcation, termination, crossover, and lake, as well as third-level details, namely sweat pores. b) Variation of the gray value over a few papillary ridges indicated by the solid white rectangle shown in (a).

average difference of around 100. Moreover, the second-level details, such as the ridge bifurcation, termination, crossover, and lake, could be clearly distinguished. These details make the fingerprint unique and form the basis of personal identification. Additionally, the third-level details, namely the sweat pores, are also observed along the papillary ridges (in magnified images), which have been known to be useful in the identification of partial or damaged fingerprints.

The deposition of a silver layer was also examined by SEM and EDS measurements. As shown in Figure 2a, the pristine hIgG-inked fingerprint does not display any characteristics, while after incubation with a solution of AuNPs/anti-hIgG conjugates for 15 minutes, the immobilization of the conjugates onto the fingerprint residue can be clearly observed (Figure 2b), with the ridges appearing bright against the dark substrate. However, in the magnified image, the AuNPs are only loosely distributed on the ridges and do not form a compact layer. A similar result was also obtained when the fingerprint was only treated with the silver staining solution (Figure 2c). In contrast, after the iMMD development, the fingerprint ridges were coated with a compact layer of silver particles that were aggregated and intertwined

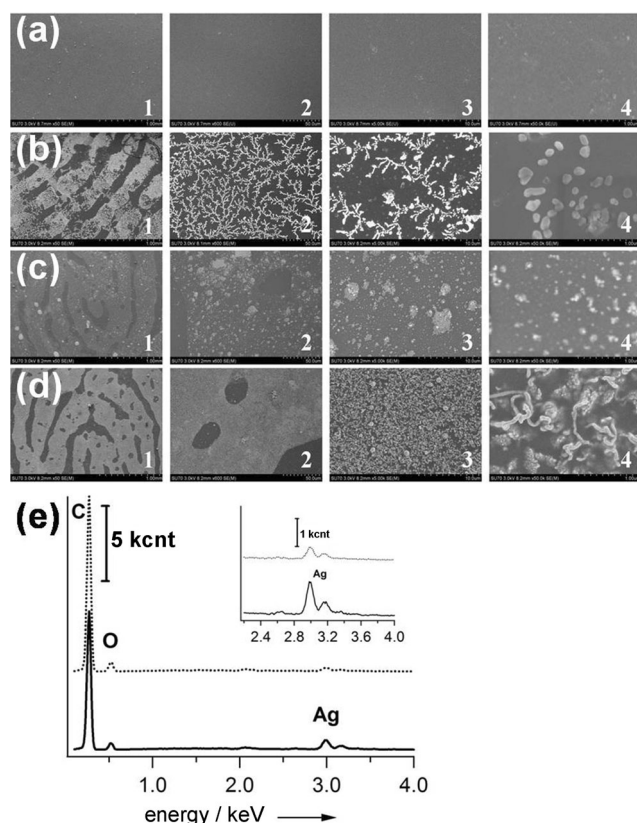


Figure 2. a–d) Scanning electron microscopy (SEM) images of hIgG-linked fingerprints before (a) and after development with only AuNPs/anti-hIgG (b), only silver staining (c), and iMMD (d). The magnification is 50 (1), 600 (2), 5000 (3) and 50000 (4). e) Energy-dispersive X-ray spectroscopy (EDS) analysis of the developed fingerprint: the solid and dotted lines correspond to the responses from the ridge and background surface, respectively. kcnt = kilocounts.

(Figure 2d). Meanwhile, the EDS image shows that the silver staining takes place predominately on the ridges, while it was insignificant on the bare tape surface, suggesting that the silver staining is indeed catalyzed by pre-adsorbed AuNPs on the residues (Figure 2e).

To estimate the sensitivity of AuNPs/anti-hIgG, we ran a semiquantitative experiment using hIgG-linked fingerprints prepared with different amounts of hIgG. The detection limit was found to reach nanograms per fingerprint, as shown in Figure S5.

Sweat contains 98–99 % water, a number of inorganic salts (such as chloride and phosphate), and organic materials (such as amino acids, fatty acids, urea, and polypeptides).^[16,17] Among various components present in sweat fingerprints, proteins/polypeptides are highly useful for the detection of biomarkers with medical or diagnostic values. However, because of the low sample concentration and high background interferences of the chemical imaging techniques, the identification of proteins/peptides is still limited and only a few kinds of them have been identified until now.^[18] As a result of its specificity (demonstrated above), iMMD is particularly suitable for providing chemical information regarding the secretions in the fingerprint residues and, at

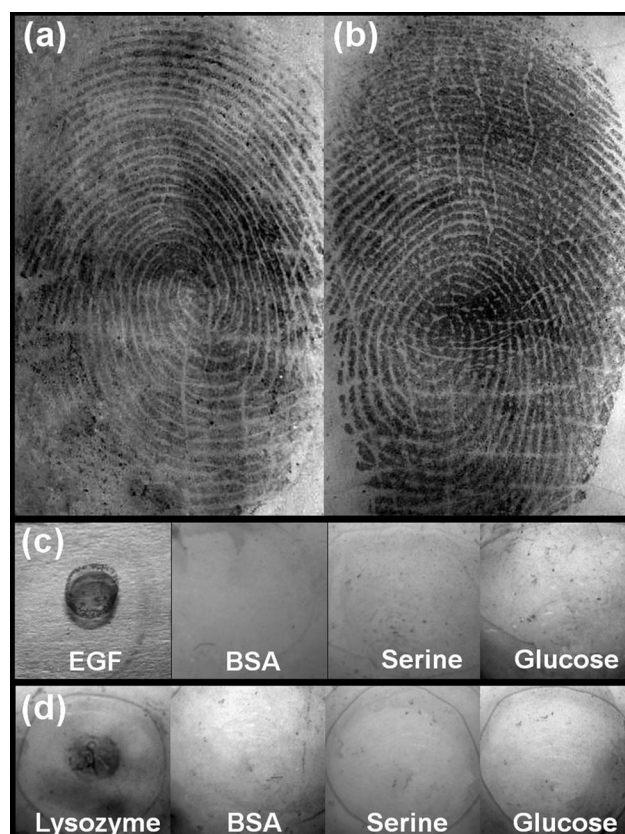


Figure 3. a,b) Optical images of eccrine sweat fingerprints visualized by iMMD through the detection of a) epidermal growth factor (EGF) and b) lysozyme. The concentration of AuNPs/antibody conjugates was 0.1 mg mL⁻¹. c) Demonstration of the selectivity of AuNPs/anti-EGF through the specific binding with EGF at 250 ng scale and the lack of binding with BSA, serine and glucose at 10 µg scale. d) Evaluation of the selectivity of AuNPs/anti-lysozyme to lysozyme through the specific binding with lysozyme at 100 ng scale and the lack of binding with BSA, serine, and glucose at 10 µg scale.

the same time, allowing the identification of an individual, by properly choosing AuNPs modified by specific antibodies. To exemplify the applicability of the proposed iMMD in the detection of target secretions in sweat fingerprints, two polypeptides were selected as the target analytes. Displayed in Figure 3a,b are the optical images of sweat fingerprints enhanced by iMMD through the detection of epidermal growth factor (EGF) and lysozyme. EGF is a low-molecular-weight polypeptide with 53 amino acid residues, which plays important roles in cellular growth, proliferation, differentiation, and survival.^[19] It has been found in the human sweat secreted by the eccrine glands. Lysozyme is an antimicrobial peptide secreted by the human sweat eccrine glands as a part of innate host defense of immune systems, which can damage the cell wall of Gram-positive bacteria by cleaving the β1→4 glycosidic bond between *N*-acetylmuramic acid and *N*-acetyl-D-glucosamine.^[20] Apparently, from each image we can successfully identify the respective polypeptide and simultaneously visualize the ridge details with bare eyes.

To prove that the enhancement is indeed due to the specific binding of AuNPs/antibody conjugates with the

respective polypeptide, spot tests were performed on standards for BSA and a number of other fingerprint components (serine, glucose, EGF, and lysozyme). Small amounts of each standard (10 µg for BSA, serine, glucose, 250 ng for EGF, and 100 ng for lysozyme) in solution were dropped onto the professional forensic tape and left to dry. Then the spots were incubated with AuNPs/anti-EGF or AuNPs/anti-lysozyme conjugates and subsequently treated with silver staining solution. As shown in Figure 3c and Figure 3d, the selectivities of AuNPs/anti-EGF and AuNPs/anti-lysozyme are demonstrated by the specific binding with only EGF and lysozyme but not with the other standards. Moreover, clear visualization of the EGF standard at 250 ng and the lysozyme standard at 100 ng scale also highlights the sensitivity of iMMD (see Figure 3c,d).

In summary, we reported a method termed iMMD for both the visualization of latent fingerprints and detection of secretions in human perspiration by combining the conventional MMD with the immunoassay technique. In comparison to conventional MMD, AuNPs not only serve as the nucleation sites for autometallographic deposition of silver particles from the silver staining solution, but also as the carriers of recognition molecules. Using hIgG as a test protein, we obtained the optimal formulation of iMMD, which was then successfully applied to visualize latent fingerprints through the detection of two secreted polypeptides, EGF, and lysozyme. In comparison with the conventional MMD, iMMD is faster and has better sensitivity and specificity. Moreover, the developed fingerprints can be directly observed with bare eyes, without involving any sophisticated or expensive instruments for detection. In addition, the method may become useful for the detection of substances of abuse, as many orally ingested and metabolized drugs are excreted in sweat. Further work is in progress to detect other species, as well as to discover potential, valuable relationships between the fingerprint components and their donors.

Received: April 17, 2014

Revised: June 4, 2014

Published online: July 30, 2014

Keywords: fingerprints · gold nanoparticles · immunology · multimetal deposition · polypeptides

- [1] a) C. Champod, C. J. Lennard, P. Margot, M. Stoilovic, *Fingerprints and other ridge skin impressions*, CRC, Boca Raton, Florida, **2004**; b) H. Faulds, *Nature* **1880**, 22, 605.
- [2] C. J. Polson, *J. Crim. Law Criminol.* **1950**, 41, 495–517.
- [3] a) D. Maio, A. K. Jain, *Handbook of fingerprint recognition*, 2nd ed., Springer, Amsterdam, **2009**; b) H. C. Lee, R. R. E. Gaensslen, *Advances in fingerprint technology*, 2nd ed., CRC, Boca Raton, Florida, **2001**.
- [4] a) O. S. Wolfbeis, *Angew. Chem.* **2009**, 121, 2302–2304; *Angew. Chem. Int. Ed.* **2009**, 48, 2268–2269; b) P. Hazarika, D. A. Russell, *Angew. Chem.* **2012**, 124, 3582–3589; *Angew. Chem. Int. Ed.* **2012**, 51, 3524–3531.
- [5] X. Shan, U. Patel, S. Wang, R. Iglesias, N. Tao, *Science* **2010**, 327, 1363–1366.
- [6] a) D. R. Ifa, N. E. Manicke, A. L. Dill, G. Cooks, *Science* **2008**, 321, 805–805; b) H.-W. Tang, W. Lu, C.-M. Che, K.-M. Ng, *Anal. Chem.* **2010**, 82, 1589–1593; c) R. Bradshaw, R. Wolstenholme, R. D. Blackledge, M. R. Clench, L. S. Ferguson, S. Francese, *Rapid Commun. Mass Spectrom.* **2011**, 25, 415–422; d) L. Ferguson, R. Bradshaw, R. Wolstenholme, M. Clench, S. Francese, *Anal. Chem.* **2011**, 83, 5585–5591; e) S. J. Hinder, J. F. Watts, *Surf. Interface Anal.* **2010**, 42, 826–829; f) R. Wolstenholme, R. Bradshaw, M. R. Clench, S. Francese, *Rapid Commun. Mass Spectrom.* **2009**, 23, 3031–3039.
- [7] a) P. Ng, S. Walker, M. Tahtouh, B. Reedy, *Anal. Bioanal. Chem.* **2009**, 394, 2039–2048; b) T. Chen, Z. D. Schultz, I. W. Levin, *Analyst* **2009**, 134, 1902–1904; c) R. Bhargava, R. Schwartz Perlman, D. Fernandez, I. Levin, E. Bartick, *Anal. Bioanal. Chem.* **2009**, 394, 2069–2075.
- [8] W. Song, Z. Mao, X. Liu, Y. Lu, Z. Li, B. Zhao, L. Lu, *Nanoscale* **2012**, 4, 2333–2338.
- [9] a) P. Hazarika, S. M. Jickells, K. Wolff, D. A. Russell, *Anal. Chem.* **2010**, 82, 9150–9154; b) P. Hazarika, S. M. Jickells, D. A. Russell, *Analyst* **2009**, 134, 93–96; c) P. Hazarika, S. M. Jickells, K. Wolff, D. A. Russell, *Angew. Chem.* **2008**, 120, 10321–10324; *Angew. Chem. Int. Ed.* **2008**, 47, 10167–10170; d) R. Leggett, E. E. Lee-Smith, S. M. Jickells, D. A. Russell, *Angew. Chem.* **2007**, 119, 4178–4181; *Angew. Chem. Int. Ed.* **2007**, 46, 4100–4103.
- [10] M. Wood, P. Maynard, X. Spindler, C. Lennard, C. Roux, *Angew. Chem.* **2012**, 124, 12438–12440; *Angew. Chem. Int. Ed.* **2012**, 51, 12272–12274.
- [11] K. Li, W. Qin, F. Li, X. Zhao, B. Jiang, K. Wang, S. Deng, C. Fan, D. Li, *Angew. Chem.* **2013**, 125, 11756–11759; *Angew. Chem. Int. Ed.* **2013**, 52, 11542–11545.
- [12] J. Wang, T. Wei, X. Li, B. Zhang, J. Wang, C. Huang, Q. Yuan, *Angew. Chem.* **2014**, 126, 1642–1646; *Angew. Chem. Int. Ed.* **2014**, 53, 1616–1620.
- [13] G. Saunders, C. Cards, in 74th Conference of the International Association for Identification, Pensacola, USA, **1989**, pp. 14–16.
- [14] a) B. Schnetz, P. Margot, *Forensic Sci. Int.* **2001**, 118, 21–28; b) A. Becue, C. Champod, P. Margot, *Forensic Sci. Int.* **2007**, 168, 169–176; c) M. Sametband, I. Shweky, U. Banin, D. Mandler, J. Almog, *Chem. Commun.* **2007**, 1142–1144.
- [15] a) S. Shenawi, N. Jaber, J. Almog, D. Mandler, *Chem. Commun.* **2013**, 49, 3688–3690; b) N. Jaber, A. Lesniewski, H. Gabizon, S. Shenawi, D. Mandler, J. Almog, *Angew. Chem.* **2012**, 124, 12390–12393; *Angew. Chem. Int. Ed.* **2012**, 51, 12224–12227.
- [16] P. J. Wood in *Understanding immunology*, 2ednd ed Pearson Education, Upper Saddle River, New Jersey, **2006**.
- [17] A. Girod, R. Ramotowski, C. Weyermann, *Forensic Sci. Int.* **2012**, 223, 10–24.
- [18] a) V. Drapel, A. Becue, C. Champod, P. Margot, *Forensic Sci. Int.* **2009**, 184, 47–53; b) L. S. Ferguson, F. Wulfert, R. Wolstenholme, J. M. Fonville, M. R. Clench, V. A. Carolan, S. Francese, *Analyst* **2012**, 137, 4686–4692; c) A. D. Reinholz, *J. Forensic Identif.* **2008**, 58, 524–539; d) A. van Dam, K. A. van Nes, M. C. Aalders, T. G. van Leeuwen, S. A. Lambrechts, *Anal. Methods* **2014**, 6, 1051–1058.
- [19] a) G. Carpenter, S. Cohen, *Annu. Rev. Biochem.* **1979**, 48, 193–216; b) A. Kasselberg, D. N. Orth, M. E. Gray, M. T. Stahlman, *J. Histochem. Cytochem.* **1985**, 33, 315–322.
- [20] a) D. C. Phillips, *Proc. Natl. Acad. Sci. USA* **1967**, 64, 483; b) M. Papini, S. Simonetti, S. Franceschini, L. Scaringi, M. Binazzi, *Arch. Dermatol. Res.* **1981**, 272, 167–170.